Toxicon 101 (2015) 41–47

Contents lists available at ScienceDirect

Toxicon

journal homepage: www.elsevier.com/locate/toxicon

A saxitoxin-binding aptamer with higher affinity and inhibitory activity optimized by rational site-directed mutagenesis and truncation

X. Zheng [a], B. Hu [a, b], S.X. Gao [a], D.J. Liu [a, b], M.J. Sun [a], B.H. Jiao [a, b], L.H. Wang [a, *]

[a] Department of Biochemistry and Molecular Biology, College of Basic Medical Sciences, Second Military Medical University, No. 800, Xiangyin Rd., Shanghai 200433, People's Republic of China
[b] Center of Marine Biolical Medicine, College of Marine Military Medicine, Second Military Medical University, No. 800, Xiangyin Rd., Shanghai 200433, People's Republic of China

ARTICLE INFO

Article history:
Received 11 January 2015
Received in revised form
9 April 2015
Accepted 29 April 2015
Available online 1 May 2015

Keywords:
Aptamer
Saxitoxin
Mutagenesis
Truncation
Inhibitory activity
G-quadruplex

ABSTRACT

Saxitoxin (STX), a member of the family of paralytic shellfish poisoning toxins, poses toxicological and ecotoxicological risks. To develop an analytical recognition element for STX, a DNA aptamer (APT^{STX1}) was previously discovered via an iterative process known as Systematic Evolution of Ligands by Exponential Enrichment (SELEX) by Handy et al. Our study focused on generating an improved aptamer based on APT^{STX1} through rational site-directed mutation and truncation. In this study, we generated the aptamer, M-30f, with a 30-fold higher affinity for STX compared with APT^{STX1}. The Kd value for M-30f was 133 nM, which was calculated by Bio-Layer Interferometry. After optimization, we detected and compared the interaction of STX with aptamers (APT^{STX1} or M-30f) through several techniques (ELISA, cell bioassay, and mouse bioassay). Both aptamers' STX-binding ability was demonstrated in all three methods. Moreover, M-30f performs better than its parent sequence with higher suppressive activity against STX. As a molecular recognition element, M-30f has good prospects for practical application.

1. Introduction

Saxitoxin (STX), with the molecular formula $C_{10}H_{17}N_7O_4$ (Molecular Weight = 299), is one of the most potent natural neurotoxins known; it is highly polar due to the presence of two guanidinium groups (Fig. 1, Wiese et al., 2010). Along with dozens of analogues, STX makes up a family of neurotoxins, which are classified as paralytic shellfish toxins (PSTs), and may cause paralytic shellfish poisoning (PSP; Etheridge, 2010). As reported, STX can be synthesized by multiple species of cyanobacteria and dinoflagellates (Perreault et al., 2011). *In vivo* accumulation of STX by filter-feeding bivalves and fish, and the subsequent transfer through the food chain, can result in human illnesses or even death (Cusick and Sayler, 2013). STX is toxic mainly because of its effect on the nervous system, where it blocks voltage-gated sodium channel in excitable cells (Tian et al., 2014). Its LD_{50} in mice is 8–10 μg kg^{-1} *i.p.*, 3.4 μg kg^{-1} *i.v.* and 260 μg kg^{-1} by oral administration (Falconer, 2008). These data demonstrates the importance of monitoring programs for STX. In many countries, the regulatory limit for PSP toxins in shellfish has been established as 800 μg of STX equivalents/kg of shellfish meat or 4 mouse unit (MU) of PSP toxins/g of shellfish meat (Kawatsu et al., 2014).

The longstanding regulatory method for validating biological threats is the internationally accredited AOAC biological method (Mouse bioassay 959.08), with only the United Kingdom using the relatively newly accredited AOAC Official HPLC Method 2005.06 as an alternative (Campbell et al., 2009). However, a rapid, high throughput screening assay for effective monitoring is still needed, which could also reduce animal usage. The most important part of a screening assay is its recognition element, e.g., the antibodies and receptors that are usually adopted (Handy et al., 2013). However, many challenges remain, e.g., the limited availability of antibodies and the use of animals. Handy et al. (2013) reported the discovery of a DNA aptamer named APT^{STX1} that targets STX, which could serve as an alternative analytical recognition element in diagnostic assays for STX (Fig. 2; Handy et al., 2013).

Aptamers are short strands of DNA or RNA that can fold into unique three-dimensional structures and bind with high affinities and specificities to targets such as ions, proteins, low molecular weight metabolites, sugar moieties, lipids, and even whole cells (Kong and Byun, 2013). They are typically screened out from a

* Corresponding author.
E-mail address: wsh928@hotmail.com (L.H. Wang).

http://dx.doi.org/10.1016/j.toxicon.2015.04.017
0041-0101/

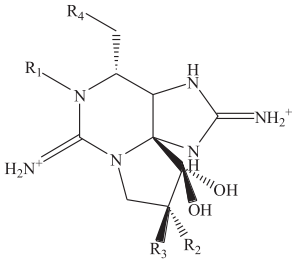

Fig. 1. Structure of STX.

random library comprising 10^{12}–10^{15} oligonucleotide sequences that are synthesized in vitro by a SELEX process (Systematic Evolution of Ligands by Exponential Enrichment) (Radom et al., 2013; Shigdar et al., 2013). Because of their numerous advantages compared to antibodies, e.g., stability and non-immunogenicity, aptamers are promising for detection and clinical applications (Wang et al., 2011). To date, several aptamers have entered clinical trials as antagonists, agonists or targeting molecules in drug delivery; the most successful one, pegaptanib, has been approved by the FDA for the treatment of vascular ocular disease (Radom et al., 2013). There has also been considerable progress towards applications of aptamers for laboratory techniques and medical diagnostics (Radom et al., 2013).

However, primary aptamers obtained by SELEX are not suitable for direct clinical or laboratory application. Optimization is needed to improve and regulate their functions (Wang et al., 2011). In recent years, a number of attempts have been made to optimize present aptamers through several common strategies, e.g., truncation, chemical modification, LNA replacement, mutation and 3' or 5' capping (Wang et al., 2011; Yang et al., 2011; Nonaka et al., 2013; Bullock et al., 2000; Pasternak et al., 2011). In this study, we adopted rational site-directed mutagenesis and truncation to optimize APT^{STX1}. First, we introduced mutations to improve its conformational stability and strengthen its interaction with STX. Although a number of aptamers have been identified by SELEX, it sometimes fails to identify aptamers that bind with their target with high affinity, because of amplification bias of PCR and reduced library diversity caused by experimental manipulation (Nonaka et al., 2013). Different groups have engineered mutated aptamers that bind to targets with improved affinity compared to the wild type (Nonaka et al., 2013; Bullock et al., 2000). Similarly, by introducing site-directed mutations on the basis of secondary structure prediction, we attempted to get an improved underlying aptamer with higher affinity. It is known that G-quadruplexes are nucleic acids structures, characterized by unique highly ordered architecture and high stability (Ruttkay-Nedecky et al., 2013). Some sequences remain folded under physiological conditions and at temperatures above 90 °C (Ruttkay-Nedecky et al., 2013). Therefore, we presume that if an aptamer can form a G-quadruplex after slight mutation, its affinity could be improved based on its strengthened structural stability. We designed experiments to verify our hypothesis. As expected, we obtained a mutated quadruplex-forming aptamer with higher affinity to STX compared to the parent aptamer. Subsequently, we adopted truncation to reduce the cost of the molecule and find the key binding structure. Generally, not all nucleotides of a certain aptamer are necessary for direct interaction with the target or for folding into the structure that facilitates target binding. Moreover, longer sequences result in lower yield and higher cost of synthesis (Shangguan et al., 2007). Thus, truncation is necessary during the optimization process. At the same time, it aids in exploring the relationship between the aptamer structure and function and in characterizing the target binding motif.

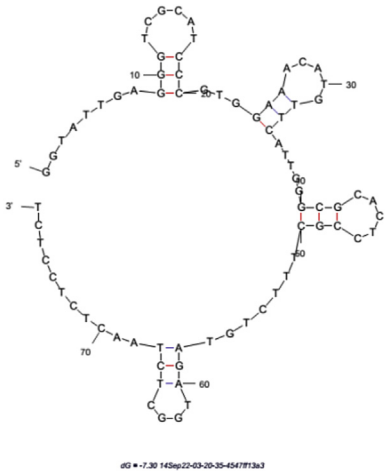

Fig. 2. Structure of APT^{STX1} generated by the mfold web server.

After optimization of aptamer APT^{STX1}, we investigated the interaction of the pre- and post-optimized aptamers with STX through different methods: ELISA, a cell bioassay and mouse bioassay. By these methods, STX was detected as a control following standard procedures. After the introduction of aptamers in these detection systems, differences could be observed compared to controls, which verified aptamers' ability of binding with STX. Besides, we compared the performances of different aptamers in these assays. Through these three methods, we obtained an overall understanding of their STX-binding ability and function.

2. Experimental

2.1. Materials and reagents

All synthetic oligonucleotides were synthesized by Sangon Biotech (Shanghai, China). STX diacetate was purchased from Taiwan Algal Science Inc (Taiwan). Ultrafiltration tubes used were Amicon Ultra-0.5 mL and Ultra-4 mL centrifugal desalting filters with a 3 KD molecular cutoff, obtained from EMD Millipore (Alberta, Canada). Ouabain(10 mM, aqueous) and Veratridine (1 mM, in 0.01 M HCl) were purchased from Sigma–Aldrich Co. LLC(mainland, China). Nuclease free water (IDT) was used in the preparation of all reagents used for experiments. PBS-T used was 10 mM phosphate buffer, 2.7 mM KCl, 140 mM NaCl, 0.05% Tween-20, pH 7.4 (Sigma, St. Louis, MO). All other chemical reagents used were analytical grade.

2.2. Evaluation of STX-aptamers binding using Bio-Layer Interferometry sensors

STX-aptamers binding was evaluated using Bio-Layer Interferometry sensors in an OctetRED 96 system (ForteBio, Shanghai). The principle and analysis procedures used herein were as detailed in Concepcion et al. (2009). Briefly, aptamer immobilization was performed using the streptavidin-biotin coupling method. SSA(enhanced streptavidin) sensors (ForteBio) were prepared by the procedure of equilibration (1 min), biotinylated aptamer coupling(1 μM, 5 min), dissociation(5 min), and equilibration (2 min); One reference channel was also prepared via equilibration. The running buffer used for immobilization and sample analysis was PBS-T at room temperature. Lyophilized aptamers were reconstituted in PBS-T to a concentration of 100 μM, then diluted in PBS-T to 10 μM and 1 μM, heated at 95 °C for 5 min, and cooled on ice for 10 min prior to use. All aptamers used for experiments herein were required to undergo the heating and cooling procedure

to promote their refolding. STX at different concentrations (5 μM, 10 μM and 20 μM) was analyzed for association time over 5min and dissociation time over 5 min, along with a blank sample containing only running buffer for reference. In addition, GTX2 and GTX3 (gonyautoxin, 20 μM) were used to evaluate the interaction of aptamers with similar paralytic shellfish toxins. The response data from the control surface were subtracted from the responses obtained from the reaction surface using the Octet Data Analysis Software CFR Part 11 Version 6.x; the affinity parameter Kd was similarly obtained. A 1:1 binding mode with mass transfer fitting was used to obtain the kinetic data.

2.3. Optimization of APT^{STX1}

During the optimization process, single-point mutations were first introduced into the sequence of the STX-binding aptamer (APT^{STX1}). A set of 22 oligonucleotide single-point mutants were obtained with mutation sites at both sides of guanine bases, since sets of guanine bases are necessary for G-quadruplex structures. The sequences of all mutants produced are listed in Table S-1, Supporting information. Prediction by QGRS Mapper revealed that 9 sequences (M-6, M-8, M-12, M-13, M-15, M-20, M-22, M-30 and M-32) among the 22 mutants could form G-quadruplex structures. To verify our hypothesis that aptamers with G-quadruplex structures could exhibit improved target affinities, the 9 sequences and the parent sequence were synthesized and their STX-binding abilities were evaluated by Bio-Layer Interferometry. Similarly, multi-point mutagenesis was also attempted. 6 quadruplex-forming multi-point mutant sequences were synthesized and their *Kd* values calculated. Ultimately, M-30 was found to have the strongest STX affinity. To remove redundant nucleotides on M-30, we conducted truncation analysis according to predictions from the mfold web server. 6 truncated sequences derived from M-30 (M-30a, M-30b, M-30c, M-30d, M-30e; Fig. 4), with bases at either ends truncated or one of four stem-loop structures removed, were synthesized and their *Kd* values were calculated by Bio-Layer Interferometry. In combination with QGRS Mapper prediction results, we were able to determine the core functional sequence of M-30 without affecting its affinity (M-30f).

2.4. ELISA

ELISA kits for the analysis of STX were purchased from Abraxis LLC (Warminster, U.S.A). The kits employ a direct competitive ELISA, coated with a second antibody (sheep anti-rabbit). STX in the sample and an STX-enzyme-conjugate compete for the binding sites of rabbit anti-STX antibodies in solution. The STX antibodies are then bound by the second antibody immobilized on the plate.

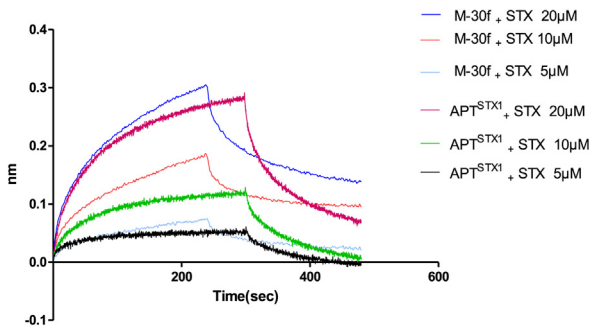

Fig. 3. Bio-Layer Interferometry association and dissociation curves. Sensors were immobilized with oligonucleotides (M-30f or APT^{STX1}). Different phase shifts to the interference spectrum were induced by different concentrations of STX (20 μM, 10 μM and 5 μM).

After a washing step and addition of the substrate solution, a color signal is produced. The intensity of the blue color is inversely proportional to the concentration of the STX present in the sample. The color reaction is terminated after a specified time and the absorbance at 450 nm was measured using a Thermo Scientific Multiskan FC Microplate Photometer. Each sample, control or standard solution was analyzed in duplicate.

In order to study the interaction of STX with M-30f or APT^{STX1}, we detected STX (0.8 ng/ml) as a control and the mixture of STX and an aptamer as a sample after incubation for 30 min at room temperature (0.8 ng/ml STX; 10^{-6}, 10^{-7} and 10^{-8} mol/L aptamers). Then, we conducted statistic analysis of the results to find out whether the introduction of aptamers could lead to changes in absorbance at 450 nm. However, no significant differences were observed among aptamer groups and control. Since STX also exists in enzyme conjugate (enzyme-STX), aptamers might bind with not only free STX but also enzyme-STX, leading to negative results above. To avoid the interference from enzyme-STX, we detected free STX remaining after incubation with an aptamer and ultrafiltration (0.5 mL, 3 KD, 14,000 rpm, 30 min). Aptamers and aptamer-STX complexes were retained in the concentrate by ultrafiltration. The free STX in the mixture of aptamer and STX was tested following the same procedure as detailed above. The efficiency of ultrafiltration was verified by denaturing polyacrylamide gel electrophoresis to confirm that aptamers and the aptamer-STX complex were not filtrated. Besides, to demonstrate that STX alone can be completely filtrated, we also designed ELISA experiments. Pre- and post-filtrated STX were both detected as samples and compared.

2.5. Cell bioassay

Neuro-2a cells (mouse neuroblastoma cells, ATCC CCL-131) were grown in RPMI 1640 complete medium (Hyclone, South America) supplemented with 10% fetal bovine serum, 2 mM glutamine, 1 mM sodium pyruvate, 50 μg/ml streptomycin, and 50 units/ml penicillin. The culture was maintained at 37 °C in a humidified CO_2 (5%) atmosphere (Humpage et al., 2007). For the bioassay, 96-well microplates were seeded with 200 μL complete medium RPMI 1640 containing 10^5 cells per well and then incubated for 24 h. Culture wells were then filled with 10 μl each of sample, 10 mM ouabain, and 1 mM veratridine. Mixture of STX (3.2, 0.8, or 0.2 ng/well) and aptamer (10^{-7} mol/L, M-30f or APT^{STX1}) after incubation was subjected to replicates of 3 wells as samples, with STX (3.2, 0.8, or 0.2 ng/well) alone as controls. 6 wells were processed as untreated controls (without additions of sample, ouabain, and veratridine) or as ouabain/veratridine controls (without addition of sample). After incubation for 24 h, the medium was wicked off with sterilized paper-towels. The wells were then given 200 μL fresh medium and 20 μL CCK-8, and incubated for another 45–60 min. Finally, the absorbance was measured with a Thermo Scientific Multiskan FC Microplate Photometer at a wavelength of 450 nm (Manger et al., 1995).

2.6. Mouse bioassay

A mouse bioassay was performed according to the official method of the Association of Analytical Communities (AOAC) (2005). We aimed to adopt this standard method to study and compare the interaction of STX with aptamers pre- and post-optimization. Briefly, the assay for PSP toxins is performed as follows: Five or more female ICR mice weighing 19.6 ± 0.4 g (approximately 4 weeks old) were intravenously (i.v.) injected with 300 μL of sample, and the survival ratio was observed. Mice were first randomly assigned to one of five treatment groups: mixture of

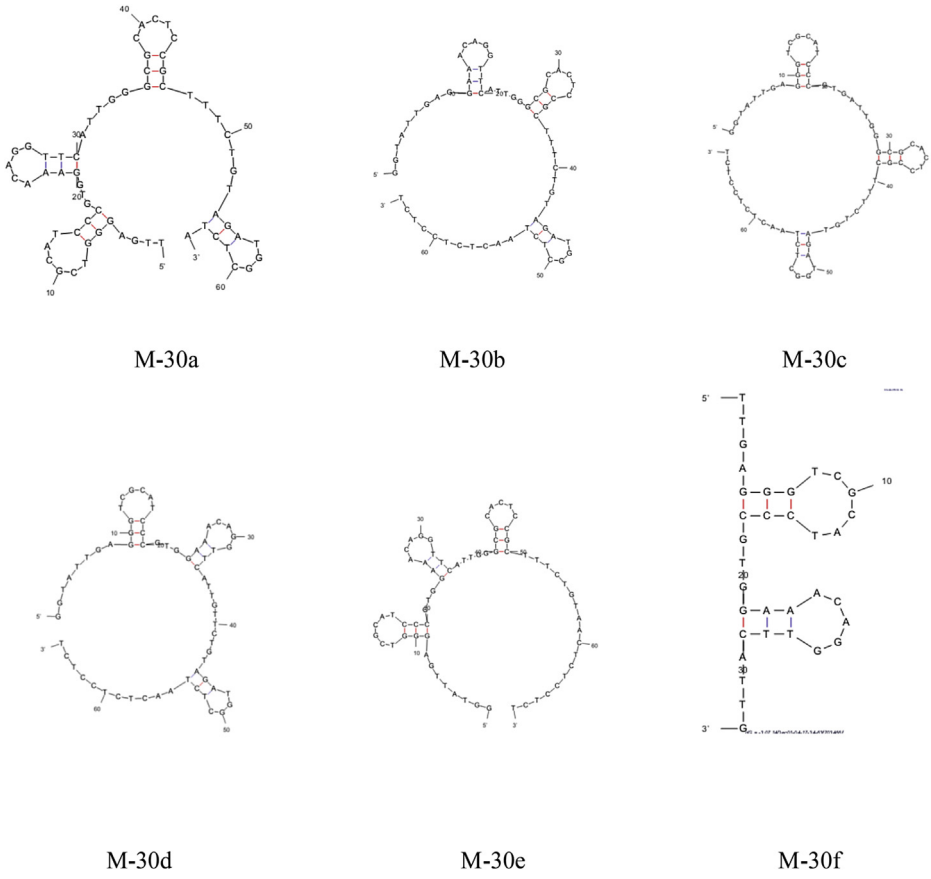

Fig. 4. Secondary structure of truncated aptamers.

STX and APT^{STX1} [4.95 mg/kg] after incubation; mixture of STX and M-30f [4.95 mg/kg] after incubation; aptamer (APT^{STX1} or M-30f) alone, and STX alone as a control. The concentration of STX suitable for use as the control was first researched prior to performing the bioassays. However, in the complicated environment in vivo, aptamers didn't protect mice from death. With the aid of ultrafiltration, mice were randomly assigned to one of following treatment groups: ultrafiltration separated STX after incubation with APT^{STX1} [4.95 mg/kg]; ultrafiltration separated STX after incubation with M-30f [4.95 mg/kg], ultrafiltration separated STX alone as a control. By ultrafiltration, in vivo interference to the interaction of aptamers with STX was avoided.

2.7. Statistics

GraphPad Prism (GraphPad Software, San Diego, CA, USA) was used for all statistical tests. Statistical significance was accepted at $p \leq 0.05$.

3. Results

3.1. Improvement of aptamer STX-binding ability through rational site-directed mutagenesis and truncation

Aptamers with high STX-binding ability are required for use as recognition elements in STX-detection systems. The affinity of an STX-binding aptamer (APT^{STX1}) that was identified in a previous study[12] was re-evaluated by Bio-Layer Interferometry. Bio-Layer Interferometry is a label-free technology. Once the molecule bound to the sensor surface fluctuates in number, the spectrometer captures the real-time phase shift of the interference spectrum, which directly reflects the thickness of the bio-layer. To date and to our knowledge, no reported studies have measured the interaction of aptamers with small molecules using Bio-Layer Interferometry. As shown in Fig. 3, increasing concentrations of STX elicited corresponding increases in the sensor response. As a negative control, running buffer was exposed to the reference channel, and no change in response was observed (data not shown); as such, non-specific binding of STX to the sensor was ruled out. By global fitting of the responses of three concentrations of STX over the oligonucleotide surface of constant density, we obtained the association–dissociation curves and the Kd values for the interactions. The curves revealed that the association and dissociation rates were both slow; therefore, aptamers needed to be incubated with STX for 30 min in our study to obtain a sufficient binding reaction. With a *Kd* value of 3.84 μM for the STX-APT^{STX1} interaction, it was evident that the binding ability of APT^{STX1} required improvement in order to construct a sensitive STX-detection system. Moreover, studies to determine specificity of the APT^{STX1} sensor surface for STX versus its congeners (GTX2 and GTX3), that often co-occur in regions where STX may be present, followed the same assay procedures. Binding response was not observed, thus indicating that APT^{STX1} didn't cross-react with GTX2 or GTX3(data not shown) and further supporting that the selected aptamer, APT^{STX1}, was specific to STX.

In the optimization process for aptamer APT^{STX1}, we first introduced individual point mutations. In the 22 resultant single-point mutants, nine sequences (M-6, M-8, M-12, M-13, M-15, M-20, M-22, M-30 and M-32) were predicted to form G-quadruplex structures based on QGRS Mapper. By Bio-Layer Interferometry, the association and disassociation parameters of each oligonucleotide

were determined and are shown in Table 1. The results signify that M-6, M-8, M-13 and M-22 have similar affinities for STX as APT^{STX1}, whereas M-12, M-15, M-20 and M-32 have reduced affinities for STX. However, one mutant shows stronger binding to STX: M-30 (5′-GGTATTGAGGGTCGCAT CCCGTGGAAACAGGTTCATTGGGCGCAC TCCGCTTTCTGTAGATGGCTCTAACTCTCCTCT-3′). The Kd value for M-30 was 128 nM, indicating that it had a 30-fold stronger binding ability than APT^{STX1}. The dissociation rate constant (K_{dis}) for M-30 was $1.54 \times 10^{-3}(s^{-1})$, whereas the K_{dis} for APT^{STX1} was 1.87×10^{-2} (s^{-1}). The association rate constant (K_{on}) for M-30 was $1.20 \times 10^{4}(M^{-1}\ s^{-1})$, whereas that for APT^{STX1} was 4.87×10^{3} ($M^{-1}\ s^{-1}$). Therefore, the improvement in STX-binding ability was mainly accomplished by increase of the association rate constant and reduction of the dissociation rate constant. Prediction by the mfold web server revealed that M-6, M-8, M-13, M-22, which maintained similar affinities for STX, had the same secondary structures from APT^{STX1}, whereas M-12, M-15, M-20 and M-32, which had reduced affinity, formed different stem-loop structure as APT^{STX1}. From these results, we conclude that both the G-quadruplex and stem-loop structure in M-30 are involved in its interaction with STX.

We next attempted multi-point mutagenesis on the basis of the results detailed above. Six additional mutants were synthesized and evaluated by Bio-Layer Interferometry. Results revealed that the affinity increased five folds at most with multi-point mutants (Table S-2, Supporting information), and all were lower than that of M-30. We speculated that aptamer M-30, with its single point mutation at site 30, showed the strongest STX-binding ability because of its particular size and the positioning of the mutation for G-quadruplex formation. Therefore, we chose M-30 as the aptamer for further optimization.

Not every nucleotide may be necessary for the STX-binding ability of M-30. We therefore conducted a truncation analysis to reduce the cost for synthesis and find the minimal functional core structure of M-30. Since stem-loop structures were involved in the interaction of aptamers with STX, five truncated sequences of M-30 (M-30a, M-30b, M-30c, M-30d, M-30e) were synthesized according to prediction from the mfold web server and their *Kd* values were determined (Table 2). Sequences M-30a, M-30d and M-30e, with bases at both ends, the third stem-loop and the fourth stem-loop structures separately removed, were found to have Kd values very close to that of the full-length M-30. However, the removal of the first or the second stem-loop from M-30 (M-30b, M-30c) resulted in dramatically reduced binding affinity, suggesting that the two stem-loop structures were critical for target recognition. According to the information generated by QGRS Mapper on the composition and distribution of putative quadruplex-forming sequences in M-30, we found that the core nucleotides for a G-quadruplex were located just in the first and second stem-loop structures. Based on these results and our inference, sequence M-30f was synthesized with the third and fourth stem-loop structures removed and redundant nucleotides at both ends truncated. As expected, its affinity was similar as that of the full-length M-30. Thus, we took M-30f as the final optimized STX-binding aptamer. Moreover, no response was observed when GTX 2 and GTX3 (20 μM) were used as targets, which indicated that M-30f did not cross-react with GTX2 or GTX3(data not shown) and maintained its specificity for STX.

Table 1
List of quadruplex-forming sequences and their kinetic parameters.

Names	*Kd*(μM)	K_{on}(1/Ms)	K_{dis}(1/s)
APT^{STX1}	3.84	4.87×10^{3}	1.87×10^{-2}
M-6	4.27	3.47×10^{3}	1.48×10^{-2}
M-8	3.50	3.04×10^{3}	1.06×10^{-2}
M-12	51.0	3.29×10^{2}	1.68×10^{-2}
M-13	3.28	4.63×10^{3}	1.52×10^{-2}
M-15	39.3	4.97×10^{2}	1.95×10^{-2}
M-20	29.1	4.13×10^{2}	1.2×10^{-2}
M-22	4.17	1.27×10^{3}	5.28×10^{-3}
M-30	0.128	1.20×10^{4}	1.54×10^{-3}
M-32	24.0	8.76×10^{2}	2.1×10^{-2}

Table 2
Kinetic parameters of truncated aptamers.

Names	*Kd*(μM)	K_{on}(1/Ms)	K_{dis}(1/s)
M-30a	0.131	1.53×10^{4}	2.00×10^{-3}
M-30b	13.8	1.62×10^{3}	2.24×10^{-2}
M-30c	10.4	2.74×10^{3}	2.85×10^{-2}
M-30d	0.137	2.15×10^{4}	2.95×10^{-3}
M-30e	0.143	1.37×10^{4}	1.96×10^{-3}
M-30f	0.133	1.40×10^{4}	1.86×10^{-3}

3.2. M-30f interacts with STX better than APT^{STX1} (ELISA)

In order to evaluate the interaction of STX with aptamers (M-30f and APT^{STX1}), we first adopted the ELISA method. With STX filtrated as a control, the mixture of STX and an aptamer after incubation was added as a sample. However, there is no significant statistic difference among aptamer groups and control. After some analysis, we speculated that the negative results were caused by aptamers' ability of binding with both free STX and enzyme-STX. To avoid the potential interference from enzyme-STX, STX separated by ultrafiltration (0.5 mL, 3KD, 14,000 rpm, 30 min) after incubation with aptamers (M-30f or APT^{STX1}) of different concentrations was subjected to the ELISA kit. The addition of aptamers, both M-30f and APT^{STX1}, resulted in a decrease in absorbance at 450 nm, which can be attributed to a reduction in the amount of free STX in the assay. In addition, at the concentrations of 10^{-7} and 10^{-6} M, absorbance decrease at 450 nm caused by M-30f was more than that caused by APT^{STX1}. Upon comparison between the M-30f and APT^{STX1} groups, statistically significant differences could be observed ($p < 0.05$, Fig. 5).

In order to verify the efficiency of ultrafiltration, STX alone was separately added to the ELISA kit, before and after ultrafiltration. Similar absorbance at 450 nm was obtained without significant difference. This demonstrates that STX could completely pass through the ultrafiltration membrane. We also verified the efficiency of ultrafiltration for DNA aptamers by denaturing

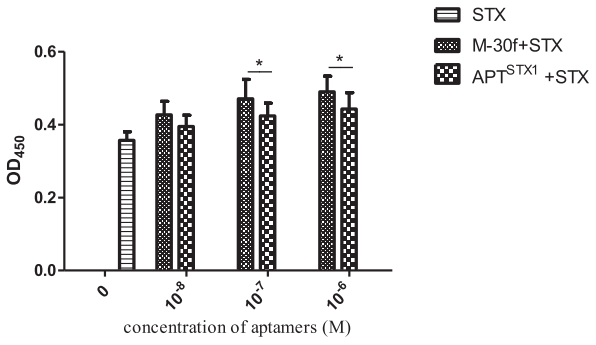

Fig. 5. Comparison of two aptamers' STX-binding ability by ELISA. STX (0.8 ng/ml) alone was taken as a control. After interaction with aptamers(M-30f and APT^{STX1}) at different concentrations (10^{-8}, 10^{-7} and 10^{-6} M), remaining free STX was obtained by filtration and added to the analyte solution. Free STX was reduced by the addition of aptamers. A significant difference was observed between M-30f and APT^{STX1} groups. (*$p < 0.05$).

polyacrylamide gel electrophoresis. APT^{STX1} before ultrafiltration exhibited a light band, while the filtrate revealed nothing, indicating that ultrafiltration could almost completely retain aptamers (≥20 KD) in the concentrate (Fig. S-1, Supporting information).

3.3. Improved inhibitory activity for M-30f compared to APT^{STX1} (cell bioassay)

The cell bioassay for STX is based on its ability to block sodium channels (Melegari et al., 2012). Veratridine and ouabain, which are known as sodium channel agonists and sodium pump inhibitors separately, reduce cell viability by 50%–74% (mean, 62%). The effect of added STX is shown by the standard curve in Fig. S-2. Neither Ouabain nor veratridine alone had fatal effect on Neuro-2a cells.

With STX as the control, mixture of STX and aptamer after incubation was subjected as a sample in cell bioassay. Then, different groups and the control were brought into comparison. As shown in Fig. 6, addition of M-30f or APT^{STX1} along with STX resulted in decreased cell viability, compared to control. What's more, significant difference ($p < 0.05$) was observed between M-30f and APT^{STX1} groups. From these results, we can conclude that both aptamers could interact with STX, and the suppression of sodium channel activity by STX was also inhibited by M-30f and APT^{STX1}, with the M-30f performing better.

3.4. M-30f and APT^{STX1} can both interact with STX (mouse bioassay)

In order to evaluate the interaction of STX with M-30f or APT^{STX1} *in vivo*, we adopted the mouse bioassay method. First, we determined a suitable concentration of STX to use as a control. The number of survivors decreased as the dose of toxin was raised (Table S-3). A lethal effect of STX was observed in five out of six mice when given 300 μL of STX (11.25 μg/kg, *i.v.*); this concentration was subsequently used in the following study. Then, 4.95 mg/kg aptamers alone or mixed with STX was administered to mice. Aptamers alone were not lethal to mice; however, in the STX mixture groups, aptamers did not protect mice from death. To study the effect of aptamers on the amount of free STX, we filtrated the mixture before injection. STX of the same concentration pre- or post ultrafiltration was injected into mice to verify the efficiency of ultrafiltration and no difference was observed, which was consistent with the results obtained above in ELISA. STX preprocessed by incubation with aptamers(M-30f or APT^{STX1}) and ultrafiltration didn't cause death to mice, which indicated that a portion of the STX was maintained in the concentrate in the form of complexes with the aptamers (Table 3). Although a difference between M-30f and APT^{STX1} at the animal level was not observed, both M-30f and APT^{STX1} showed high affinity towards STX and resulted in the direct reduction of the STX dose administered to mice.

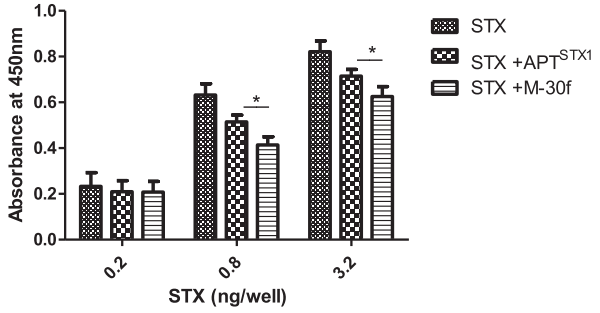

Fig. 6. Comparison of two aptamers' STX-binding ability in cell bioassay. STX alone (0.2, 0.8 and 3.2 ng/well) was used as the controls. After interaction with aptamers(M-30f and APT^{STX1}, 10^{-7} M), aptamer-STX mixtures were added to the analyte solution. Cell survival was reduced by the addition of the mixtures. A significant difference was observed between M-30f and APT^{STX1} groups. (*$p < 0.05$).

4. Discussion

In this study, we obtained a significantly improved STX-binding aptamer (M-30f) with higher affinity (30-fold) and inhibitory activity than the parent aptamer identified by SELEX (APT^{STX1}). It is well known that the secondary structure of oligonucleotides affects the amplification efficiency of PCR. Therefore, oligonucleotides with higher order structures may not be easily amplified in SELEX, which reduces the efficiency of obtaining aptamers with high target-binding ability through this technique. Thus, post-SELEX optimization is necessary to find potential sequences with desired properties. As demonstrated in this study, site-directed mutagenesis is a promising strategy for continued aptamer optimization.

The relation between structure and function was also researched in our study. To reduce the cost of synthesis and remove unnecessary nucleotides, the length of aptamer M-30f was truncated to only 34 nucleotides. We find that the core target-binding structure is formed by the first and second stem-loops, which is consistent with the assumption by Handy et al. (2013) that the primer-binding section is involved in the binding reaction. Additionally, these two stem-loop structures can form a G-quadruplex, as predicted by QGRS Mapper. It is assumed that STX-binding aptamers can form a pocket for binding of small marine toxin; the formation of a G-quadruplex might tighten the interaction of the pocket with STX, which results in a slower dissociation rate and higher affinity as observed.

Finally, using a range of techniques (ELISA, cell bioassay and mouse bioassay), we compared the STX-binding abilities of M-30f and APT^{STX1}. All the results demonstrate that both M-30f and APT^{STX1} can bind STX, though M-30f shows increased binding compared to APT^{STX1} in the ELISA and cell bioassays. Moreover, both aptamers showed STX inhibitory activity in the cell bioassay, whereas the same phenomenon was not observed in mice. This difference is probably due to the aptamers' inadequate nuclease stability in serum, a topic for further research in the future.

As a recognition molecule for STX, M-30f has great potential for practical application. For monitoring programs, a compact Bio-Layer Interferometry sensor can be researched and developed, allowing for real-time and high-throughput detection, with M-30f as a molecular recognition element for STX. With high affinity and good selectivity, M-30f may be able to outcompete antibodies in STX diagnostics. It is anticipated that the use of M-30f in STX detection methods could reduce or eliminate animal-based models, as well as the numerous challenges associated with antibody-based methods. Furthermore, M-30f can also be adopted to filter STX from ocean water to protect human from paralytic shellfish poisoning. For clinical applications, M-30f still needs to be further optimized to improve and regulate its functions and in vivo behaviors such as stability, bio-distributions, blood clearances, etc. This may be done

Table 3
STX toxicity after interaction with aptamers and filtration. STX and aptamers were used at concentrations of 11.25 μg/kg and 4.95 mg/kg, respectively.

Saxitoxin	M-30f	APT^{STX1}	Alive/tested
+	+	−	6/6
+	−	+	6/6
+	−	−	1/6
−	+	−	6/6
−	−	+	6/6

through more diverse optimization methods, e.g., phosphorothioate internucleotide linkages, 2′-O-CH_3 nucleotide modification, 5'-modified pyrimidines and LNA replacement. Such modifications may be applied to STX-binding aptamers as the aim of future research.

Acknowledgments

The authors would like to thank Professor Wang for guidance and review of the manuscript, and the National Science Foundation for the funding for the work (Chinese High-Tech R&D (863) Program, 2013AA092904).

Conflict of interest statement

The authors declare no competing interests.

Transparency document

Transparency document related to this article can be found online at http://dx.doi.org/10.1016/j.toxicon.2015.04.017.

Appendix A. Supplementary data

Supplementary data related to this chapter can be found at http://dx.doi.org/10.1016/j.toxicon.2015.04.017.

References

AOAC, 2005. AOAC Official Method 959.08, pp. 79–80.

Bullock, T.L., Sherlin, L.D., Perona, J.J., 2000. Tertiary core rearrangements in a tight binding transfer RNA aptamer. Nat. Struct. Biol. 7 (6), 497–504. http://dx.doi.org/10.1038/75910.

Concepcion, J., Witte, K., Wartchow, C., Choo, S., Yao, D., Persson, H., Wei, J., Li, P., Heidecker, B., Ma, W., Varma, R., Zhao, L.S., Perillat, D., Carricato, G., Recknor, M., Du, K., Ho, H., Ellis, T., Gamez, J., Howes, M., Phi-Wilson, J., Lockard, S., Zuk, R., Tan, H., 2009. Label-free detection of biomolecular interactions using BioLayer interferometry for kinetic characterization. Comb. Chem. High Throughput Screen 12 (8), 791–800. Available at: http://www.ncbi.nlm.nih.gov/pubmed/19758119.

Campbell, K., Huet, A.-C., Charlier, C., Higgins, C., Delahaut, P., Elliott, C.T., 2009. Comparison of ELISA and SPR biosensor technology for the detection of paralytic shellfish poisoning toxins. J. Chromatogr. B Anal. Technol. Biomed. Life Sci. 877 (32), 4079–4089. http://dx.doi.org/10.1016/j.jchromb.2009.10.023.

Cusick, K.D., Sayler, G.S., 2013. An overview on the marine neurotoxin, saxitoxin: genetics, molecular targets, methods of detection and ecological functions. Mar. Drugs 11 (4), 991–1018. http://dx.doi.org/10.3390/md11040991.

Etheridge, S.M., 2010. Paralytic shellfish poisoning: seafood safety and human health perspectives. Toxicon 56, 108–122. http://dx.doi.org/10.1016/j.toxicon.2009.12.013.

Falconer, I.R., 2008. Health effects associated with controlled exposures to cyanobacterial toxins. Adv. Exp. Med. Biol. 619, 607–612. http://dx.doi.org/10.1007/978-0-387-75865-7_27.

Humpage, A.R., Ledreux, A., Fanok, S., Bernard, C., Briand, J.F., Eaglesham, G., Papageorgiou, J., Nicholson, B., Steffensen, D., 2007. Application of the neuroblastoma assay for paralytic shellfish poisons to neurotoxic freshwater cyanobacteria: interlaboratory calibration and comparison with other methods of analysis. Environ. Toxicol. Chem. 26, 1512–1519.

Handy, S.M., Yakes, B.J., DeGrasse, J.A., Campbell, K., Elliott, C.T., Kanyuck, K.M., Degrasse, S.L., 2013. First report of the use of a saxitoxin-protein conjugate to develop a DNA aptamer to a small molecule toxin. Toxicon 61, 30–37. http://dx.doi.org/10.1016/j.toxicon.2012.10.015.

Kong, H.Y., Byun, J., 2013. Nucleic acid aptamers: new methods for selection, stabilization, and application in biomedical science. Biomol. Ther. (Seoul) 21 (6), 423–434. http://dx.doi.org/10.4062/biomolther.2013.085.

Kawatsu, K., Kanki, M., Harada, T., Kumeda, Y., 2014. A highly rapid and simple competitive enzyme-linked immunosorbent assay for monitoring paralytic shellfish poisoning toxins in shellfish. Food Chem. 162, 94–98. http://dx.doi.org/10.1016/j.foodchem.2014.04.038.

Manger, R.L., Leja, L.S., Lee, S.Y., Hungerford, J.M., Hokama, Y., Dickey, R.W., Granade, H.R., Lewis, R., Yasumoto, T., Wekell, M.M., 1995. Detection of sodium channel toxins:directed cytotoxicity assays of purified ciguatoxins, brevetoxins,saxitoxins and seafood extracts. J. AOAC Int. 78 (2), 521–527.

Melegari, S.P., Perreault, F., Moukha, S., Popovic, R., Creppy, E.E., Matias, W.G., 2012. Induction to oxidative stress by saxitoxin investigated through lipid peroxidation in Neuro 2A cells and Chlamydomonas reinhardtii alga. Chemosphere 89 (1), 38–43. http://dx.doi.org/10.1016/j.chemosphere.2012.04.009.

Nonaka, Y., Yoshida, W., Abe, K., Ferri, S., Schulze, H., Bachmann, T.T., Ikebukuro, K., 2013. Affinity improvement of a VEGF aptamer by in silico maturation for a sensitive VEGF-detection system. Anal. Chem. 85 (2), 1132–1137. http://dx.doi.org/10.1021/ac303023d.

Perreault, F., Matias, M.S., Melegari, S.P., Pinto, C.R.S.D.C., Creppy, E.E., Popovic, R., Matias, W.G., 2011. Investigation of animal and algal bioassays for reliable saxitoxin ecotoxicity and cytotoxicity risk evaluation. Ecotoxicol. Environ. Saf. 74 (4), 1021–1026. http://dx.doi.org/10.1016/j.ecoenv.2011.01.016.

Pasternak, A., Hernandez, F.J., Rasmussen, L.M., Vester, B., Wengel, J., 2011. Improved thrombin binding aptamer by incorporation of a single unlocked nucleic acid monomer. Nucleic Acids Res. 39 (3), 1155–1164. http://dx.doi.org/10.1093/nar/gkq823.

Radom, F., Jurek, P.M., Mazurek, M.P., Otlewski, J., Jeleń, F., 2013. Aptamers: molecules of great potential. Biotechnol. Adv. 31 (8), 1260–1274. http://dx.doi.org/10.1016/j.biotechadv.2013.04.007.

Ruttkay-Nedecky, B., Kudr, J., Nejdl, L., Maskova, D., Kizek, R., Adam, V., 2013. G-quadruplexes as sensing probes. Molecules 18 (12), 14760–14779. http://dx.doi.org/10.3390/molecules181214760.

Shangguan, D., Tang, Z., Mallikaratchy, P., Xiao, Z., Tan, W., 2007. Optimization and modifications of aptamers selected from live cancer cell lines. Chembiochem 8 (6), 603–606. http://dx.doi.org/10.1002/cbic.200600532.

Shigdar, S., Macdonald, J., Connor, M.O., Wang, T., Xiang, D., Shamaileh, H. Al., Qiao, L., Wei, M., Zhou, S., Zhu, Y., Kong, L., Bhattacharya, S., Li, C., Duan, W., August 2013. Aptamers as Theranostic Agents: Modifications, Serum Stability and Functionalisation, pp. 13624–13637 doi:10.3390/s131013624.

Tian, L., Cheng, J., Chen, X., Han, S., Ling, Y., Kwan, P., Lam, S., Lai, L., Wang, M., 2014. Toxicon early developmental toxicity of saxitoxin on medaka (Oryzias melastigma) embryos. Toxicon 77, 16–25. http://dx.doi.org/10.1016/j.toxicon.2013.10.022.

Wiese, M., D'Agostino, P.M., Mihali, T.K., Moffitt, M.C., Neilan, B.A., 2010. Neurotoxic alkaloids: saxitoxin and its analogs. Mar. Drugs 8 (7), 2185–2211. http://dx.doi.org/10.3390/md8072185.

Wang, R.E., Wu, H., Niu, Y., Cai, J., 2011. Improving the stability of aptamers by chemical modification. Curr. Med. Chem. 18 (27), 4126–4138. Available at: http://www.ncbi.nlm.nih.gov/pubmed/21838692.

Yang, Y., Ren, X., Schluesener, H.J., Zhang, Z., 2011. Aptamers: selection, modification and application to nervous system diseases. Curr. Med. Chem. 18 (27), 4159–4168. Available at: http://www.ncbi.nlm.nih.gov/pubmed/21838689.